Identification of post-transcriptional regulatory networks during myeloblast-to-monocyte differentiation transition

Giulia Fontemaggi[1], Teresa Bellissimo[2], Sara Donzelli[1], Ilaria Iosue[2], Barbara Benassi[3], Giorgio Bellotti[4], Giovanni Blandino[1,*], and Francesco Fazi[2,*]

[1]Translational Oncogenomics Unit; "Regina Elena" National Cancer Institute; Rome, Italy; [2]Department of Anatomical, Histological, Forensic, and Orthopedic Sciences; Section of Histology & Medical Embryology; Sapienza University of Rome; Rome, Italy; [3]Unit of Radiation Biology and Human Health; ENEA-Casaccia; Rome, Italy; [4]Department of Engineering; "Roma Tre" University; Rome, Italy

Treatment of leukemia cells with 1,25-dihydroxyvitamin D$_3$ may overcome their differentiation block and lead to the transition from myeloblasts to monocytes. To identify microRNA-mRNA networks relevant for myeloid differentiation, we profiled the expression of mRNAs and microRNAs associated to the low- and high-density ribosomal fractions in leukemic cells and in their differentiated monocytic counterpart. Intersection between mRNAs shifted across the fractions after treatment with putative target genes of modulated microRNAs showed a series of molecular networks relevant for the monocyte cell fate determination, as for example the post-transcriptional regulation of the Polo-like kinase 1 (PLK1) by miR-22–3p and let-7e-5p.

Introduction

During hematopoiesis the cell lineage determination of haematopoietic progenitor cells (HPCs) is largely controlled by a unique combination of lineage specific transcription factors (TFs) that regulate in a cooperative way the activity of promoters and enhancers present on their target genes.[1,2] Interestingly, recent findings indicate that microRNAs (miRNAs) also are involved in the regulation of the haematopoietic cell fate determination at different stages.[3] For example, in human CD34+HPCs undergoing unilineage differentiation/maturation the miR-223 overexpression favors granulocytic differentiation, whereas, the miRNAs 17–5p-20a-106a knockdown results in a more rapid monocytic differentiation.[4,5] Moreover, it is clearly emerging that miRNAs are integrated with transcription factors in regulatory circuitries involved in the decisions regarding the ability to self-renew and to generate a differentiated progeny in haematopoietic cells including myeloid cells.[6-9]

Acute myeloid leukemia (AML) represents the clonal expansion of haematopoietic precursors blocked at different stages of differentiation and several evidences link the deregulated miRNAs expression to the establishment of the leukemic phenotype highlighting a role for miRNAs in hematopoiesis and tumorigenesis.[10] Of note, the maturation block underlying specific AML subtypes may be efficiently overcome in vitro and ex vivo by the treatment with physiologic inducers such as the active form of vitamin D, 1,25-dihydroxyvitamin D$_3$ [1,25(OH)$_2$D$_3$] that is able to trigger human myeloid precursors differentiation.[11-13]

Given the relevance of miRNAs activity in pathological hematopoiesis many efforts are focused to disclose the gene expression regulatory networks established by miRNAs during the onset of

the leukemic phenotype and the differentiation treatment of AML.[10,14,15]

miRNAs are able to modulate gene expression mainly by tuning the rate of proteins' translation.[16-20] Recent studies present evidence that miRNAs may repress protein synthesis inhibiting initiation or later stages of translation.[21-25] However, it has been also recently reported that destabilization of target mRNAs may also be responsible for reduced protein output.[26,27]

Prediction algorithms usually provide hundreds of target genes for each miRNA and the identification of reliable target genes is feasible only through single-gene approaches. To identify relevant miRNA targets, implicated in the differentiation of AML cells, we here evaluated the localization of miRNAs and mRNAs in ribosomal/polysomal cell fractions obtained by sucrose density gradient centrifugation from the acute myeloblastic leukemia cell line HL60 induced or not to differentiate by 1,25-dihydroxyvitamin D$_3$ treatment to induce monocyte/macrophage differentiation.[28] A change in the association of an mRNA with polysomes is indicative of changes in its translation state. For instance, a block in translational initiation would result in reduced ribosome density on the affected mRNA and a shift toward the lower-density fractions of the gradient. On this basis we took advantage of mRNA/miRNA expression information across the low- and high-density ribosomal fractions to identify reliable target mRNAs of miRNAs relevant for monocyte differentiation.

Results and Discussion

To identify relevant miRNAs-mRNAs functional interactions during monocytic differentiation of AML cells, we performed microarray analyses of the ribosome/polysome-associated miRNAs and mRNAs in proliferating HL60 cells and in cells induced to differentiate by 1,25-dihydroxyvitamin D$_3$ (VitD$_3$) treatment. A schematic representation of the experimental approach is presented in **Figure 1A**. Monocytic differentiation of HL60 cells was assessed by CD14/CD11b surface markers analysis and by NBT assay for the assessment of phagocytic and cytotoxic activity (**Fig. 1B**).

To separate fractions with different ribosomal density, cell lysates from HL60 cells, treated or not with VitD$_3$ for 72 hours, were subjected to sucrose density gradient centrifugation, obtaining 11 fractions for each experimental condition (**Fig. S1A**). The obtained fractions 3, 4 and 5 correspond to the 40S, 60S and 80S subunits, respectively, while fractions 6 to 11 correspond to polysomes. RNA was extracted from each fraction and expression profiling of miRNAs and mRNAs from fractions 3 through 11 (which enabled sufficient amplification and labeling) was performed on the Agilent (Human miRNA microarray V3) and on the Affymetrix (GeneChip Human Gene 1.0 ST Array) platforms, respectively.

A subset of miRNAs shows altered ribosomal association after monocyte differentiation

Expression profiling identified 177 miRNAs (**Fig. 1C**) that were detectable in at least 2 of the analyzed fractions. miRNAs were mainly located in low-density fractions (**Fig. 2A**). This localization suggested an involvement of miRNAs mainly in translation initiation blockage in our experimental system.

To highlight miRNAs functionally involved in translation control during monocyte/macrophage differentiation we searched for miRNAs whose association with ribosomal machinery was affected by VitD$_3$-mediated differentiation. As shown in **Figure 1D**, we identified 9 and 22 miRNAs whose association with ribosomal machinery was increased and decreased, respectively, after VitD$_3$ treatment (**File S1**). Association of 6 selected miRNAs (let-7e-5p, miR-146a-5p, miR-378a-3p, miR-22–3p, miR-96–5p and miR-17–5p) to the ribosomal fractions was validated by RT-qPCR analysis (**Fig. 1E-J**), which confirmed that these miRNAs mainly localized to the low-density fractions, where they are increased or decreased after monocytic differentiation. Interestingly, RT-qPCR analysis of such 4 miRNAs in total RNA preparations from HL60 cells, treated or not with VitD$_3$, revealed that let-7e-5p and miR-22–3p are markedly upregulated after VitD$_3$, miR-146a-5p is slightly upregulated, miR-378a-3p is undetectable, while miR-96–5p and miR-17–5p are downregulated (**Fig. 1E-J**, right graphs). This indicates that the analysis of ribosomal fractions enables the identification of potentially relevant miRNAs that wouldn't be identified through expression analysis on total RNA. To analyze lineage specificity of the observed miRNA modulations, the expression level of miRNAs that were altered in total RNA between control and VitD$_3$ treated cells was evaluated in additional differentiation conditions, as granulocytic differentiation of NB4 cells (induced by retinoic acid), monocytic differentiation of THP-1 cells (induced by TPA) and erythroid differentiation of K562 cells (induced by AraC). As shown in **Supplementary Figure 1B**, we observed that miR-22–3p, miR-96–5p and miR-17–5p show expression modulations that are common to both monocytic and granulocytic differentiation.

Among the 22 miRNAs showing lower ribosome association in differentiated cells we noticed 8 members of the miR-17–92 cluster. Down-regulation of members of miR-17–92 cluster was previously reported in TPA- and PMA-driven monocytic differentiation of AML cells.[15,29] Moreover, also members of the miRNAs showing higher ribosome association in differentiated cells in our results (such as for example miR-21–5p, miR-22–3p and miR-26a-5p) were previously shown to be upregulated during monocyte differentiation of leukemia cells.[15,29-32]

mRNAs belonging to monocyte/macrophage-related functions are modulated during the VitD$_3$-induced differentiation of HL60 cells

The analysis of the effect of differentiation on mRNAs association to ribosomal/polysomal fractions evidenced 967 genes with enhanced recruitment to the ribosomal/polysomal machinery and 545 genes with decreased recruitment after VitD$_3$ treatment (**Fig. 2A**; **File S2**).
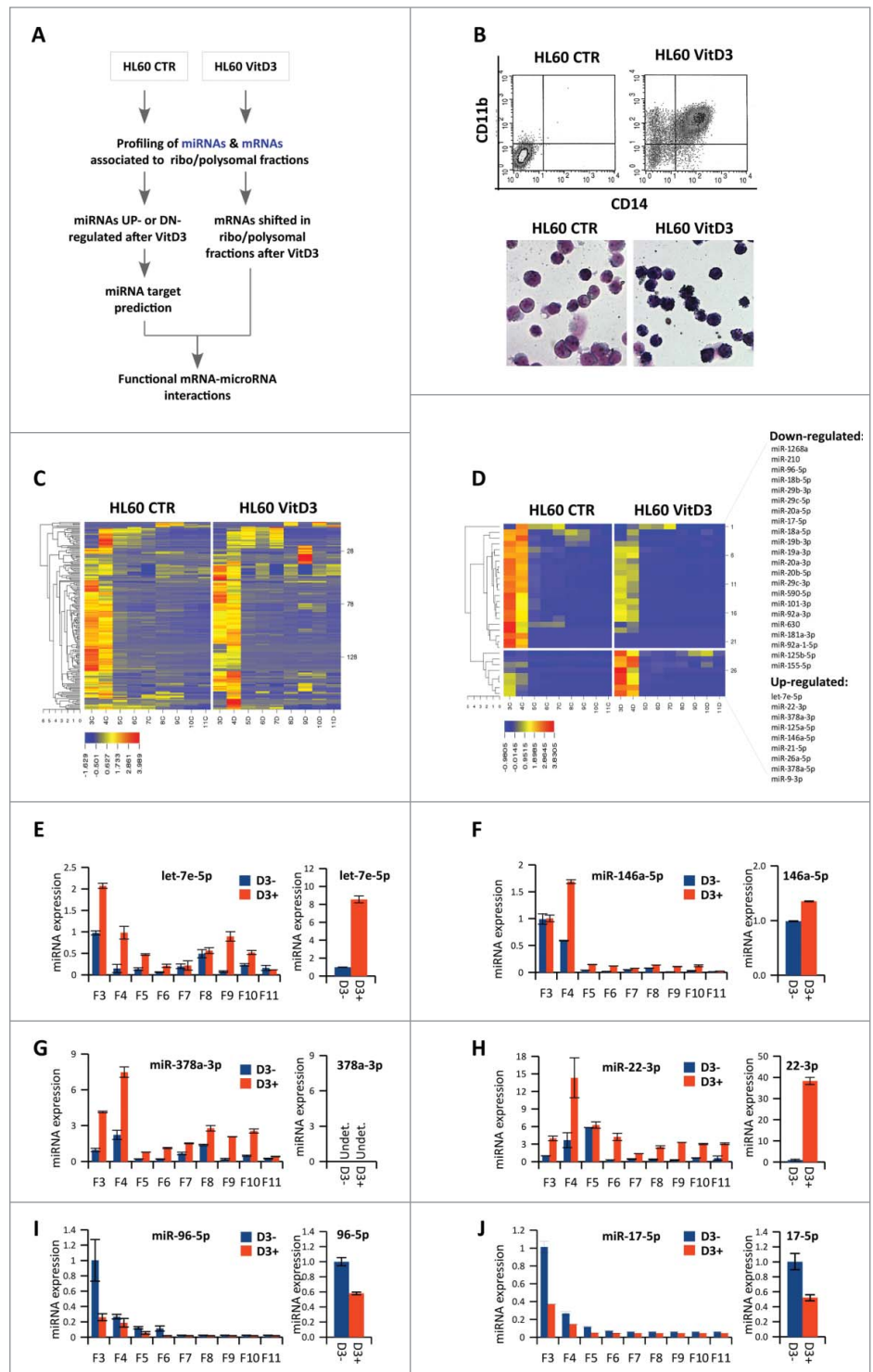
To investigate whether these modulated genes were functionally related, we performed functional annotation clustering using the DAVID bioinformatics database. As shown in **Figure 2B** and **Supplementary File 3**, among the up-regulated transcripts we

Figure 1. Expression profiles of miRNAs in the ribosomal/polysomal fractions of HL60 cells treated or not with VitD$_3$ for 72h. (**A**). Schematic representation of the experimental approach. mRNA and miRNA expression profiles were obtained from RNA associated to high- and low-density ribosomal fractions in HL60 cells treated with VitD$_3$ (HL60 VitD$_3$) or control untreated cells (HL60 CTR). mRNAs that were shifted from high- to low-density fractions and vice versa after VitD$_3$ treatment were considered for subsequent intersection analysis with the list of genes putatively targeted by VitD$_3$-modulated miRNAs to identify miRNA-mRNA interactions. (**B**). HL60 were treated (HL60 VitD$_3$) or not (HL60 CTR) for 72h with VitD$_3$ to induce monocytic differentiation. FACS analysis of cells positively stained for CD11b and CD14 myeloid surface markers (upper panel) and a light microscopy representative field showing the NBT dye reduction assay (lower panel) are shown. (**C**). Expression profile of the 177 detectable miRNAs in ribosomal/polysomal fractions from HL60 cells treated or not with VitD$_3$ for 72 h. (**D**). Expression profile of 22 and 9 miRNAs respectively down- and up-regulated by treatment of HL60 cells with VitD$_3$ for 72 h. (**E-J**). RT-qPCR analysis of 6 selected miRNAs, let-7e-5p, miR-22–3p, miR-146a-5p, miR-378a-3p, miR-96–5p and miR-17–5p, in ribosomal/polysomal fractions from HL60 cells treated or not with VitD$_3$ for 72 h. Each graph on the right shows RT-qPCR analysis of that miRNA in total RNA from HL60 cells treated or not with VitD$_3$ for 72 h.

identified a significant enrichment for genes belonging to pathways strictly related to well-known monocyte/macrophage functions, as chemokines and cytokines signaling, phagocytosis and various receptors signaling pathways (Toll like-, NOD like-, and RIG-1 like- receptors). According to the reduced proliferation that is observed during HL60 differentiation,[33] among the down-regulated transcripts we found a significant enrichment for cell cycle promoting genes, such as cyclins (B1, B2 and H), CDK6 and Bub family genes (Bub1, Bub1b and Bub3) (**File S3**).

Transcripts shifting between low- and high-density fractions after VitD$_3$ treatment maybe subjected to miRNAs-mediated translation control

We reasoned that changes in the abundance of miRNAs in the low-density fractions following the differentiation of HL60 cells to monocytes/macrophages should result in changes of their target mRNAs abundance between low- and high-density fractions. Specifically, we expected that an up-regulation of a miRNA, following VitD$_3$ treatment, should result in the shift of its target mRNAs to the low-density fractions, with consequent translational repression; on the contrary, a downregulation of a miRNA should result in a shift of its target mRNAs to the high-density
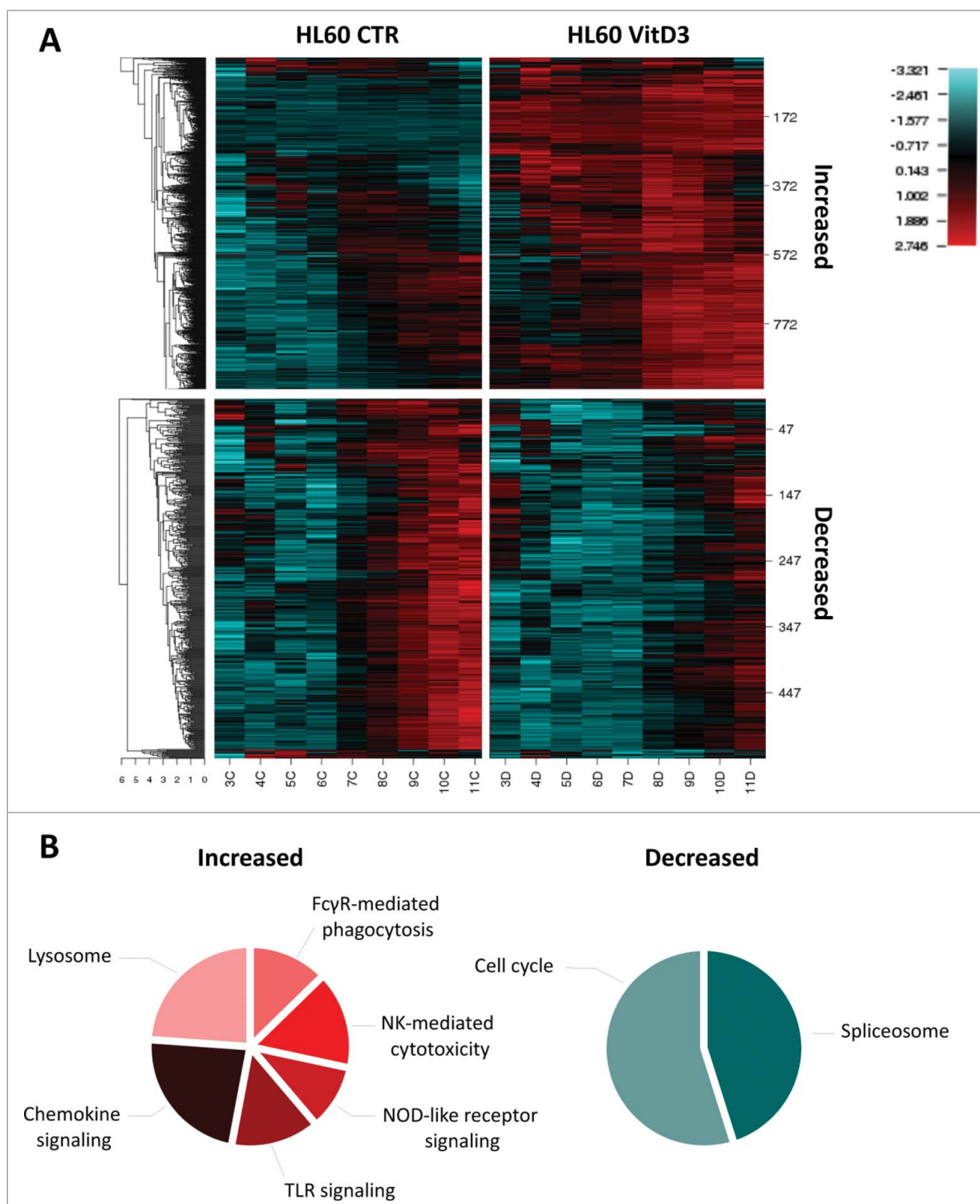
Figure 2. Expression profiles of mRNAs in the ribosomal/polysomal fractions of HL60 cells treated or not with VitD $_3$ for 72h. (**A**). Expression matrix representing the distribution across low- and high-density ribosomal fractions of mRNAs significantly modulated following VitD$_3$ treatment of HL60 cells. (**B**). Functional annotation analysis of genes modulated during differentiation of HL60 cells. Pathways with p-value <0.02 and containing >10 genes were selected.

fractions, with consequent loosening of the translational repression. On this rational basis we first sought if there were mRNAs that moved from high- to low- density fractions and vice versa following VitD₃ treatment. We thus identified 473 transcripts that were shifted from high- to low- density fractions following treatment (hereafter indicated as "slowed-down" mRNAs) and 301 transcripts that behaved in opposite manner (hereafter indicated as "speeded-up" mRNAs). A score indicating the strength of shifting between high- and low- density fractions was assigned to each of these transcripts (**Table 1; File S2**).

Functional annotation analysis of these speeded-up (SU) and slowed-down (SD) mRNAs is reported in **Figure 3A** and **Supplementary File 4**. SU mRNAs belong to processes, such as for

example "transport through vesicles" and "protein localization," which were not enriched in the increased genes shown in **Figure 1B**; on the contrary, SD mRNAs were enriched for genes belonging to processes also found in the decreased genes shown in **Figure 1B** (for example "cell cycle" and "splicing").

We validated by RT-qPCR the distribution of some of these transcripts among the ribosomal fractions. As shown in **Figures 3B-D**, we observed a shift of the mRNAs encoding KPNA2, SF2A1 and PLK1 from the high-density to the low-density fractions following treatment with VitD₃. On the contrary RAB5C and RAB10 mRNAs behaved in opposite manner, shifting from the low-density to the high-density fractions after VitD₃ (**Fig. 3E; Fig. S2A**).

Table 1. miRNAs predicted to target the top 20 ranked speeded-up and slowed-down mRNAs

Symbol	Gene Name	Score	miRNA
top 20 ranked speeded-up mRNAs			
MLF2	myeloid leukemia factor 2	9,58	miR-125b-5p (2)
SRI	sorcin	8,53	miR-590–5p, miR-630, miR-18a-5p, miR-20a-5p, miR-18b-5p
RAB10	RAB10, member RAS oncogene family	7,83	miR-20b-5p, miR-20a-5p, miR-17–5p, miR-96–5p
POLR2K	polymerase (RNA) II polypeptide K	7,78	miR-101–3p
TRAPPC1	trafficking protein particle complex 1	7,73	miR-96–5p
INSIG2	insulin induced gene 2	7,54	miR-19a-3p, miR-20b-5p, miR-92a-3p, miR-19b-3p, miR-17–5p, miR-96–5p
DPY30	dpy-30 homolog (C. elegans)	7,47	miR-101–3p
POMP	proteasome maturation protein	6,88	miR-101–3p
PAIP2	poly(A) binding protein interacting protein 2	6,76	miR-29b-3p (3), miR-29c-3p (2), miR-96–5p
TAF12	(TBP)-associated factor, 20kDa	6,76	miR-96–5p
AP1S1	adaptor-related protein complex 1, sigma 1 subunit	6,75	miR-29b-3p, miR-29c-3p
NR1H2	nuclear receptor subfamily 1, group H, member 2	6,74	miR-18a-5p, miR-18b-5p
CFL1	cofilin 1	6,72	miR-96–5p
UBE2A	ubiquitin-conjugating enzyme E2A	6,68	miR-101–3p, miR-19a-3p (3), miR-19b-3p (6)
RAB5C	RAB5C, member RAS oncogene family	6,66	miR-18a-5p (2), miR-18b-5p (2)
CDC42SE2	CDC42 small effector 2	6,63	miR-20b-5p, miR-18a-5p, miR-20a-5p, miR-18b-5p
ANAPC13	anaphase promoting complex subunit 13	6,59	miR-92a-3p
DAD1	defender against cell death 1	6,52	miR-19a-3p, miR-19b-3p
NDFIP1	Nedd4 family interacting protein 1	6,48	miR-101–3p (2), miR-19a-3p, miR-19b-3p, miR-18a-5p, miR-18b-5p
TMEM50A	transmembrane protein 50A	6,31	miR-125b-5p, miR-92a-3p
top 20 ranked slowed-down mRNAs			
KPNA2	karyopherin α 2	9,55	miR-26a-5p (2)
PLK1	Polo-like kinase 1	9,33	miR-22–3p, let7e-5p (2), miR-9–3p
RBM22	RNA binding motif protein 22	8,22	miR-21–5p
DPF2	D4, zinc and double PHD fingers family 2	7,92	miR-125a-5p, miR-22–3p, let7e-5p
DLST	dihydrolipoamide S-succinyltransferase	7,65	let7e-5p
FLII	flightless I homolog (Drosophila)	7,47	miR-125a-5p, miR-378a-3p
PES1	pescadillo homolog 1 (zebrafish)	7,39	miR-125a-5p
EFTUD2	elongation factor Tu GTP binding domain containing 2	7,36	miR-26a-5p
NMT1	N-myristoyltransferase 1	7,07	miR-125a-5p
NUSAP1	nucleolar and spindle associated protein 1	6,93	miR-22–3p
ARFGAP2	ADP-ribosylation factor GTPase activating protein 2	6,84	miR-125a-5p, miR-22–3p
DDX24	DEAD (Asp-Glu-Ala-Asp) box helicase 24	6,83	miR-22–3p
CTPS	CTP synthase 1	6,79	miR-125a-5p, let7e-5p
DPP3	dipeptidyl-peptidase 3	6,49	miR-146a-5p, let7e-5p
METTL3	methyltransferase like 3	6,46	miR-21–5p
GTPBP1	GTP binding protein 1	6,42	miR-125a-5p, miR-21–5p
ADRBK2	adrenergic, β, receptor kinase 2	6,37	miR-146a-5p, miR-26a-5p, miR-125a-5p, miR-378a-3p
GOT2	glutamic-oxaloacetic transaminase 2, mitochondrial	6,33	miR-378a-3p
NT5DC1	5'-nucleotidase domain containing 1	6,08	miR-26a-5p, miR-125a-5p, miR-378a-3p
SF3A1	splicing factor 3a	6,08	miR-26a-5p

Numbers in parenthesis, when present, indicate the number of sites for a given miRNA on target mRNA.
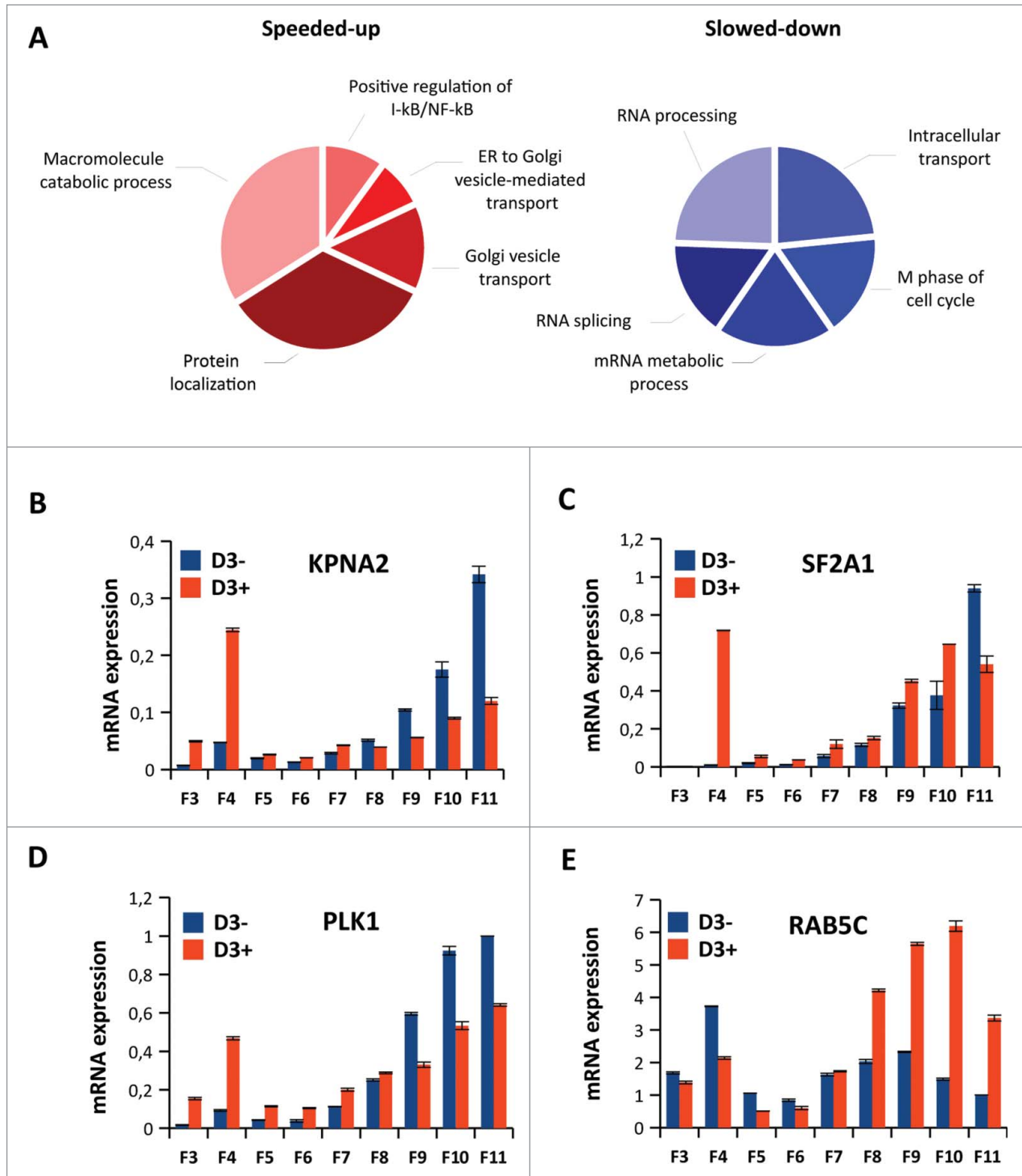
Figure 3. VitD₃ treatment leads to the shift of a group of mRNAs between high- and low-density fractions. (**A**). Functional annotation analysis of the speeded-up and slowed-down mRNAs during differentiation of HL60 cells. The most statistically significant biological processes are shown. (**B**). RT-qPCR analysis of KPNA2, SF2A1, PLK1 and RAB5C was performed on low- and high-density fractions from HL60 cells treated or not with VitD₃ for 72h. Gene expression was normalized over 18S rRNA.

Speeded-up and slowed-down transcripts are good candidates for miRNA-mediated translation control and were used for subsequent analysis.

We generated lists of putative predicted targets for each of the miRNAs altered between proliferating and differentiated HL60 cells (**Fig. 1D**). mRNAs that were predicted to be targeted by

a given miRNA by at least 3 out of 10 considered prediction algorithms were included in each list.

We intersected the list of slowed-down mRNAs with that of putative target mRNAs of upregulated miRNAs and the list of speeded-up mRNAs with that of putative target mRNAs of downregulated miRNAs. Results for the top 20 ranked speeded-up and slowed-down genes and the miRNAs predicted to target them are reported in **Table 1**. Results for all intersections are enclosed in the **Supplementary Files 5 and 6**.

We next evaluated effects of miRNAs modulation on protein expression of shifted mRNAs. Specifically, inhibition of miR-96–5p and miR-17–5p activity by transfection of LNA oligonucleotides resulted in increased expression of RAB10 protein, whose transcript was speeded-up upon differentiation and predicted to be targeted by these miRNAs (**Fig. S2A**).

While examining the shifted transcripts, our attention was particularly captured by PLK1, a major mitotic regulator, which is emerging as an attractive therapeutic target in AML.[34] PLK1 has indeed been reported to be strongly up-regulated in the majority of AML patients and, in recent years, several PLK1 inhibitors have been developed, with Volasertib showing the most promising results in early-phase clinical trials.[34,35]

According to the increased PLK1 mRNA in low-density fractions following differentiation, we observed that PLK1 protein level decreased in HL60 cells after VitD$_3$ treatment (**Fig. 4A**). Similar results were observed in the U937 cell line treated with VitD$_3$ (**Fig. 4B**).

To evaluate whether this was a miRNA-dependent down-regulation, we analyzed PLK1 protein levels in HL60 cells depleted or not of Argonaute-2 (Ago-2) protein. Argonaute-2 is the main mediator of the translation inhibitory activity of miRNAs and we previously reported that Ago-2 expression is necessary for VitD$_3$-driven monocytic differentiation.[13] As shown in **Figure 4C**, the downregulation of PLK1 protein occurring after VitD$_3$ treatment is lost in cells depleted of Ago-2, indicating the requirement of miRNAs activity for PLK1 translation control during monocytic differentiation.

As reported in **Table 1**, PLK1 mRNA is predicted to be targeted by 3 of the miRNAs that we found increased after differentiation (e.g. miR-22–3p, let-7e-5p and miR-9–3p). Functional correlation analysis of the miRNAs that were upregulated after VitD$_3$ treatment, performed using DIANA miRPath V2.0 web-server,[36] evidenced that, of the 3 miRNAs predicted to target PLK1, miR-22–3p and let-7e-5p were the most strictly related (**Fig. 4D**). Base pairing of PLK1 mRNA with miR-22–3p or let-7e-5p is shown in **Figure 4E**. We next evaluated whether modulation of expression of these miRNAs affected PLK1 expression. To this end we transfected miR-22–3p mimic, let-7e-5p mimic or control mimic in U937 cells, showing high basal levels of PLK1, and we analyzed PLK1 protein expression during differentiation. As shown in **Figure 4F** and **Supplementary Figure 2C**, miR-22–3p and let-7e-5p over-expression resulted in down-regulation of PLK1 protein expression in untreated cells (left panel) and after VitD$_3$ treatment (middle and right panels). Analysis of PLK1 mRNA levels in the same experimental conditions further supports post-transcriptional regulation of PLK1 by miR-22–3p

and let-7e-5p (**Fig. 4G**). As miR-22–3p is predicted to target PLK1 through a sequence located internally to the protein coding region (CDS) we evaluated whether miR-22–3p mimic transduction was able to down-regulate an exogenously expressed PLK1 transcript lacking 5'-UTR and 3'-UTR. As shown in **Figure 4H**, miR-22–3p mimic transduction decreases endogenous (left panel) as well as exogenous GFP-tagged (right panel) PLK1 expression to an extent similar to that observed upon VitD$_3$ treatment.

Altogether these results demonstrate that the co-localization of miRNAs and predicted target mRNAs in low-density ribosomal fractions is strongly indicative of their functional interaction.

The identification of new molecular players involved in myeloid cell fate determination paves the way for the identification of new potentially interesting molecular targets for the treatment of acute myeloid leukemia.

Materials and Methods

Cell culture and proliferation/differentiation assay

HL60, NB4, THP-1 and K562 cell lines were maintained in RPMI 1640 medium supplemented with 1 × penicillin/streptomycin solution, 1 × L-glutamine and 10% Fetal Bovine Serum. Cell proliferation and differentiation were evaluated and quantified by direct cell counting (trypan blue dye exclusion method) using a hemocytometer chamber, by NBT dye reduction assay and by direct immunofluorescence analysis for the evaluation of the CD11b-CD14 co-expression as a marker of monocytic differentiation, as previously described.[13]

Reagents

1,25-dihydroxyvitamin D$_3$ (VitD$_3$) was purchased from Sigma-Aldrich (St. Louis, MO, USA) and utilized at a concentration of 250 ng/ml.

Western blot analysis

30 μg of whole-cell extract were separated by 4–12% SDS-PAGE (Invitrogen) and electroblotted to nitrocellulose membrane (Protran, Whatman S&S, Maidstone, UK). Mouse monoclonal anti-PLK1 (Abcam, #17057), anti-Tubulin (Sigma-Aldrich), anti-GAPDH (Sigma-Aldrich) and rabbit polyclonal anti-β-Actin (Cell Signaling), anti-GFP (Santa Cruz Biotechnology, sc-9996) and anti-Rab 10 (Cell Signaling, #4262) were used. Western blot analysis was performed with the aid of the enhanced chemiluminescence system (Thermo Fisher Scientific, Rockford, IL, USA). ECL detection was done using a UVITEC Alliance 4.7 (Cambridge, UK) instrument.

Polysome analysis and fractionation

Polyribosome preparation and polysome analysis were essentially performed as previously described.[37] Briefly, 30×10^6 cells were washed with ice cold PBS and resuspended in 300 μl of ice-cold Lysis Buffer (10 mM Tris-HCl [pH 7.5], 50 mM KCl, 10 mM MgCl$_2$, 0.1% NP-40, 15 U/ml RNaseOUT, 1 mM PMSF and 1 μg/ml Aprotinin, 1 μg/ml Leupeptin), incubated
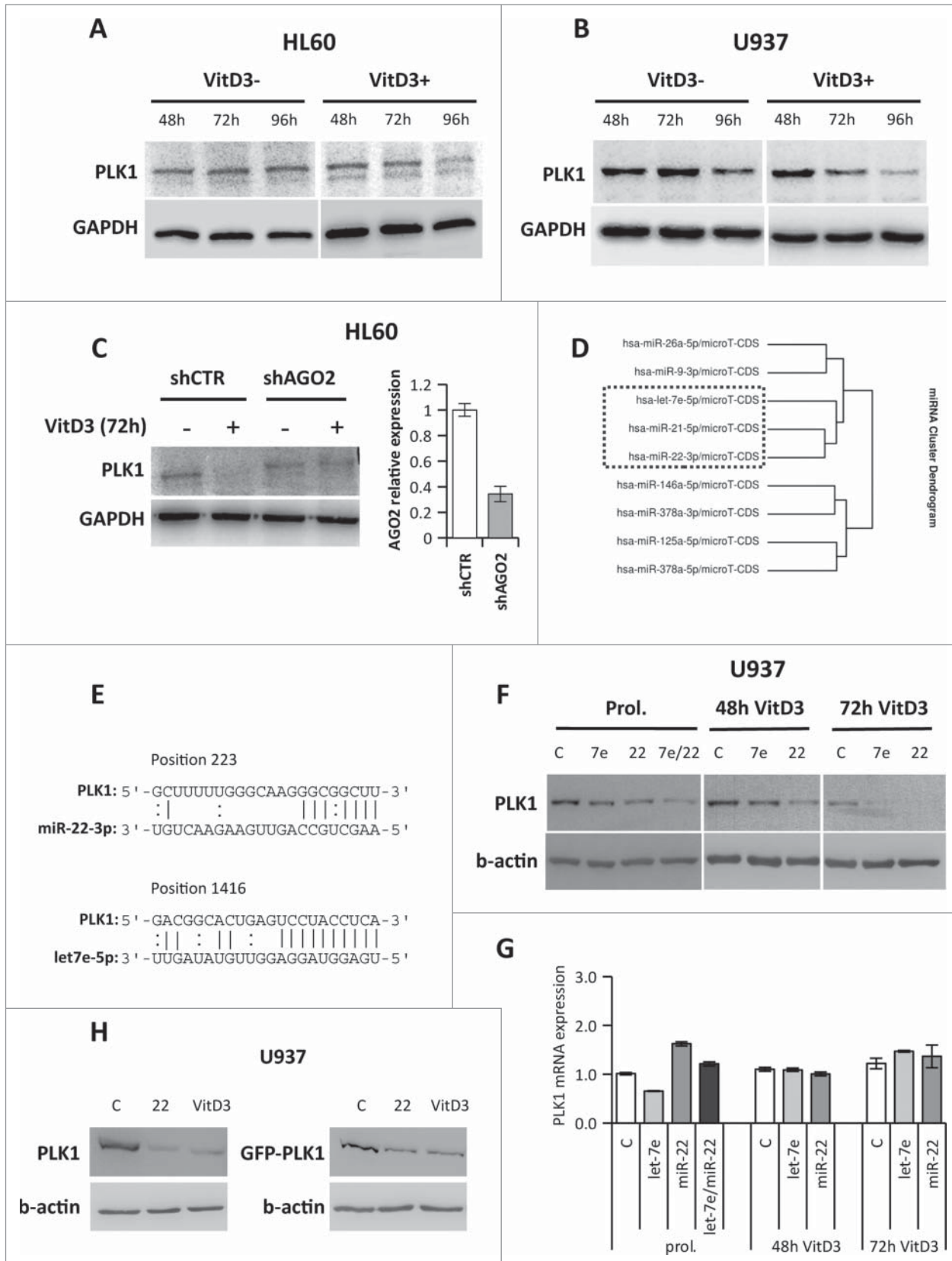
Figure 4. For figure legend, see page 698.

for 10 min on ice and centrifuged at 4°C for 10 min at 13.000 rpm. The supernatant was collected, layered on a linear 15 to 50% sucrose gradient prepared in 10 mM Tris-HCl [pH 7.5], 50 mM KCl, 10 mM $MgCl_2$ and centrifuged at 4°C in a SW41 Beckman rotor for 2h at 37.000 rpm. The gradient was scanned at A_{254} by using the BioLogic system (Bio-Rad) with a flow rate of 1.25 ml/min and fractionated by using the 2110 gradient collector (Bio-Rad) with a fix size of 0.8 ml/fraction. From each fraction the RNA sample was extracted by using TRIzol RNA Isolation Reagent (Invitrogen, Carlsbad, CA, USA).

Ago2 Silencing by Lentiviral shRNA

The shRNA expression cassette for AGO2 silencing was subcloned to generate the lentiviral vector pRRLsin.PPT.shAGO2.hPGK.EGFP.WP and the infective particles were produced and utilized as previously described.[13]

Cells transfection and treatment

3×10^5 cells/ml were transfected with mirVana mimic (Ambion) negative control or let7e-5 p or miR-22–3 p, and miR-CURY LNA^{TM} microRNA negative control or miR-96–5 p or miR-17–5 p inhibitors (Exiqon) at final concentration of 5nM in a 6-well plate using TransIT-X2® Dynamic Delivery System (Mirus) according to the manufacturer's instructions. Twenty-four hours after transfection, cells were treated with 250 ng/ml of $VitD_3$ and harvested at 48 h and 72 h of treatment.

RNA extraction and RT-qPCR

Total RNA for microarray analyses was extracted using Trizol (Invitrogen, Carlsbad, CA, USA) from fractions obtained by sucrose density gradient centrifugation. Genomic DNA contamination was eliminated through a DNase I (Qiagen, Chatsworth, CA) digestion step. RNA was further purified on Qiagen RNeasy columns for gene expression profiling (Qiagen, Chatsworth, CA). The concentration and purity of total RNA were assessed using a Nanodrop TM 1000 spectrophotometer (Nanodrop Technologies, Wilmington, DE, USA). Reverse transcription was performed with SuperScript II (Invitrogen). Quantification of miRNAs was carried out with TaqMan MicroRNA Assays (Applied Biosystems) normalizing over endogenous RNU44 snRNA. RT-qPCR was carried out on ABI PRISM 7500 Sequence Detection System (Applied Biosystems, Carlsbad, CA, USA) using assays listed in **Supplementary Table 1**. Expression values of mRNAs were calculated by standard curve method and normalized over 18S rRNA.

Expression profiling of miRNAs

Total RNA (100 ng) was labeled and hybridized to Human miRNA microarray V3 (Agilent). Scanning and image analysis were performed using the Agilent DNA Microarray Scanner (P/N G2565BA). Feature Extraction Software (Version 10.5) was used for data extraction from raw microarray image files using the miRNA_105_Dec08 FE protocol. miRNAs were called present if at least 2 of the fractions presented values over the cut-off (set at 5). miRNA expression values were considered modulated when their expression was changed more than 2 folds in fractions F3 and F4 after $VitD_3$ treatment. Expression values were standardized, so that the expression of each miRNA has mean 0 and standard deviation 1. miRNA expression values are deposited in GEO database with accession number GSE67837.

Lists of miRNAs predicted targets were generated by using the miRWalk website (http://www.umm.uni-heidelberg.de/apps/zmf/mirwalk). mRNAs predicted to be targeted by at least 3 out of 10 prediction algorithms were considered. For miRNAs not included in all prediction algorithms databases, all available programs were used.

Hierarchical clustering of miRNAs and pathways based on the levels of their interactions was performed using the DIANA miR-Path V2.0 web-server.[36]

Expression profiling of mRNAs

Expression profiles were determined by using the Human Gene 1.0 ST arrays (Affymetrix) according to the manufacturer's instructions as previously described.[38] Scanned image files (.CEL) were processed, normalized (RMA-Sketch Quantile) and Log2-transformed by Expression Console Software (Affymetrix website). Transcripts presenting values higher than 6 in at least 3 out of the 18 fractions were considered for further analyses. A supervised comparison analysis was performed by using the Analyzer software in order to select significantly modulated genes.[39] Hierarchical cluster analysis was performed using CTWC algorithm (http://ctwc.weizmann.ac.il/ctwc.htlm). mRNA expression values are deposited in GEO database with accession number GSE67837.

Definition of the score for slowed-down and speeded-up mRNAs

To identify transcripts shifted between the low- and high-density ribosomal fractions following $VitD_3$ treatment, expression signals were processes using MATLAB (The MathWorks Inc..) in house-built routines. Specifically, we selected transcripts satisfying the following conditions: $(sum(D(:,1:4)-C(:,1:4),2)>1.$ and sum$(D(:,6:9)-C(:,6:9),2)<-1.)$ i.e. the subtraction of the sum of the values of the fractions 1–4 from the untreated sample from the

---

Figure 4. (See previous page). PLK1 is down-regulated at translation level during monocyte differentiation. (**A-B**). Western blot analysis of PLK1 protein in HL60 (**A**) and U937 (**B**) cells treated or not with $VitD_3$ for the indicated times. (**C**). Western blot analysis of PLK1 protein in control and Ago2-depleted HL60 cells in presence/absence of $VitD_3$ treatment (left panel). RT-qPCR analysis of Ago-2 mRNA in control and Ago2-depleted HL60 cells is shown in right panel. (**D**). miRNA cluster dendrogram showing the functional correlation analysis of the miRNAs that were upregulated after $VitD_3$ treatment. Analysis was performed using DIANA miRPath V2.0 software. (**E**). Base pairing between PLK1 mRNA and miR-22–3p or let-7e-5p. (**F**). Western blot analysis of PLK1 protein in U937 cells transfected with let-7e-5p mimic (indicated with 7e), miR-22–3p mimic (indicated with 22) or control mimic (indicated with C), after 48h and 72 h of $VitD_3$ treatment (upper panels). (**G**). PLK1 mRNA levels from experiment shown in (**G**), evaluated by RT-qPCR. (**H**). Western blot analysis of endogenous (left panel) and exogenous GFP-tagged (right panel) PLK1 proteins in untreated U937 cells transfected with miR-22–3p mimic (indicated with 22) or control mimic (indicated with C), and in $VitD_3$-treated U937 (indicated with $VitD_3$).

sum of the VitD$_3$-treated fractions 1–4, must be greater than 1; moreover, the subtraction of the sum of the values of the fractions 6–9 from the untreated sample from the sum of the VitD$_3$-treated fractions 6–9, must be lower than −1. To transcripts that meet this condition we assigned a score defined as follows:

$$\text{Score} = (\text{sum}(D(:,1:4) - D(:,6:9), 2) + \text{sum}(C(:,6:9) - C(:,1:4), 2))$$

Gene Ontology

Enriched KEGG pathways and biological processes were identified by using the DAVID bioinformatic tool (http://david.abcc.ncifcrf.gov/home.jsp).

Disclosure of Potential Conflicts of Interest

No potential conflicts of interest were disclosed.

Supplemental Material

Supplemental data for this article can be accessed on the publisher's website.

References

1. Rosenbauer F, Tenen DG. Transcription factors in myeloid development: balancing differentiation with transformation. Nat Rev Immunol 2007; 7:105-17; PMID:17259967; http://dx.doi.org/10.1038/nri2024.

2. Orkin SH, Zon LI. Hematopoiesis: an evolving paradigm for stem cell biology. Cell 2008; 132:631-44; PMID:18295580; http://dx.doi.org/10.1016/j.cell.2008.01.025.

3. Chen CZ, Li L, Lodish HF, Bartel DP. MicroRNAs modulate hematopoietic lineage differentiation. Science 2004; 303:83-6; PMID:14657504; http://dx.doi.org/10.1126/science.1091903.

4. Vian L, Di Carlo M, Pelosi E, Fazi F, Santoro S, Cerio AM, Boe A, Rotilio V, Billi M, Racanicchi S, et al. Transcriptional fine-tuning of microRNA-223 levels directs lineage choice of human hematopoietic progenitors. Cell Death Differ 2013; 21(2):290-301; PMID:24141720.

5. Fontana L, Pelosi E, Greco P, Racanicchi S, Testa U, Liuzzi F, Croce CM, Brunetti E, Grignani F, Peschle C. MicroRNAs 17-5p-20a-106a control monocytopoiesis through AML1 targeting and M-CSF receptor upregulation. Nat Cell Biol 2007; 9:775-87; PMID:17589498; http://dx.doi.org/10.1038/ncb1613.

6. Fazi F, Nervi C. MicroRNA: basic mechanisms and transcriptional regulatory networks for cell fate determination. Cardiovasc Res 2008; 79:553-61; PMID:18539629; http://dx.doi.org/10.1093/cvr/cvn151.

7. O'Connell RM, Zhao JL, Rao DS. MicroRNA function in myeloid biology. Blood 2011; 118:2960-9; PMID:21725054; http://dx.doi.org/10.1182/blood-2011-03-291971.

8. Iwasaki H, Akashi K. Myeloid lineage commitment from the hematopoietic stem cell. Immunity 2007; 26:726-40; PMID:17582345; http://dx.doi.org/10.1016/j.immuni.2007.06.004.

9. Chen K, Rajewsky N. The evolution of gene regulation by transcription factors and microRNAs. Nat Rev Genet 2007; 8:93-103; PMID:17230196; http://dx.doi.org/10.1038/nrg1990.

10. Chen J, Odenike O, Rowley JD. Leukaemogenesis: more than mutant genes. Nat Rev Cancer 2010; 10:23-36; PMID:20029422; http://dx.doi.org/10.1038/nrc2765.

11. Nowak D, Stewart D, Koeffler HP. Differentiation therapy of leukemia: 3 decades of development. Blood 2009; 113:3655-65; PMID:19221035; http://dx.doi.org/10.1182/blood-2009-01-198911.

12. Koeffler HP, Hirji K, Itri L. One, 25-Dihydroxyvitamin D3: in vivo and in vitro effects on human preleukemic and leukemic cells. Cancer Treat Rep 1985; 69:1399-407; PMID:2416438.

13. Iosue I, Quaranta R, Masciarelli S, Fontemaggi G, Batassa EM, Bertolami C, Ottone T, Divona M, Salvatori B, Padula F, et al. Argonaute 2 sustains the gene expression program driving human monocytic differentiation of acute myeloid leukemia cells. Cell Death Dis 2013; 4:e926; PMID:24263100; http://dx.doi.org/10.1038/cddis.2013.452.

14. Fatica A, Fazi F. MicroRNA-regulated pathways in hematological malignancies: how to avoid cells playing out of tune. Int J Mol Sci 2013; 14:20930-53; PMID:24145746; http://dx.doi.org/10.3390/ijms141020930.

15. Schmeier S, MacPherson CR, Essack M, Kaur M, Schaefer U, Suzuki H, Hayashizaki Y, Bajic VB. Deciphering the transcriptional circuitry of microRNA genes expressed during human monocytic differentiation. BMC Genomics 2009; 10:595; PMID:20003307; http://dx.doi.org/10.1186/1471-2164-10-595.

16. Gebauer F, Hentze MW. Molecular mechanisms of translational control. Nat Rev Mol Cell Biol 2004; 5:827-35; PMID:15459663; http://dx.doi.org/10.1038/nrm1488.

17. Huntzinger E, Izaurralde E. Gene silencing by microRNAs: contributions of translational repression and mRNA decay. Nat Rev Genet 2011; 12:99-110; PMID:21245828; http://dx.doi.org/10.1038/nrg2936.

18. Krol J, Loedige I, Filipowicz W. The widespread regulation of microRNA biogenesis, function and decay. Nat Rev Genet 2010; 11:597-610; PMID:20661255.

19. Meister G. miRNAs get an early start on translational silencing. Cell 2007; 131:25-8; PMID:17923084; http://dx.doi.org/10.1016/j.cell.2007.09.021.

20. Valencia-Sanchez MA, Liu J, Hannon GJ, Parker R. Control of translation and mRNA degradation by miRNAs and siRNAs. Genes Dev 2006; 20:515-24; PMID:16510870; http://dx.doi.org/10.1101/gad.1399806.

21. Humphreys DT, Westman BJ, Martin DI, Preiss T. MicroRNAs control translation initiation by inhibiting eukaryotic initiation factor 4E/cap and poly(A) tail function. Proc Natl Acad Sci U S A 2005; 102:16961-6; PMID:16287976; http://dx.doi.org/10.1073/pnas.0506482102.

22. Olsen PH, Ambros V. The lin-4 regulatory RNA controls developmental timing in Caenorhabditis elegans by blocking LIN-14 protein synthesis after the initiation of translation. Dev Biol 1999; 216:671-80; PMID:10642801; http://dx.doi.org/10.1006/dbio.1999.9523.

23. Pillai RS, Bhattacharyya SN, Artus CG, Zoller T, Cougot N, Basyuk E, Bertrand E, Filipowicz W. Inhibition of translational initiation by Let-7 MicroRNA in human cells. Science 2005; 309:1573-6; PMID:16081698; http://dx.doi.org/10.1126/science.1115079.

24. Petersen CP, Bordeleau ME, Pelletier J, Sharp PA. Short RNAs repress translation after initiation in mammalian cells. Mol Cell 2006; 21:533-42; PMID:16483934; http://dx.doi.org/10.1016/j.molcel.2006.01.031.

25. Standart N, Jackson RJ. MicroRNAs repress translation of m7Gppp-capped target mRNAs in vitro by inhibiting initiation and promoting deadenylation. Genes Dev 2007; 21:1975-82; PMID:17699746; http://dx.doi.org/10.1101/gad.1591507.

26. Guo H, Ingolia NT, Weissman JS, Bartel DP. Mammalian microRNAs predominantly act to decrease target mRNA levels. Nature 2010; 466:835-40; PMID:20703300; http://dx.doi.org/10.1038/nature09267.

27. Hendrickson DG, Hogan DJ, McCullough HL, Myers JW, Herschlag D, Ferrell JE, Brown PO. Concordant regulation of translation and mRNA abundance for hundreds of targets of a human microRNA. PLoS biology 2009; 7:e1000238; PMID:19901979; http://dx.doi.org/10.1371/journal.pbio.1000238.

28. Birnie GD. The HL60 cell line: a model system for studying human myeloid cell differentiation. Br J Cancer Suppl 1988; 9:41-5; PMID:3076064.

29. Chen A, Luo M, Yuan G, Yu J, Deng T, Zhang L, Zhou Y, Mitchelson K, Cheng J. Complementary analysis of microRNA and mRNA expression during phorbol 12-myristate 13-acetate (TPA)-induced differentiation of HL-60 cells. Biotechnol Lett 2008; 30:2045-52; PMID:18648749; http://dx.doi.org/10.1007/s10529-008-9800-8.

30. Sharbati S, Sharbati J, Hoeke L, Bohmer M, Einspanier R. Quantification and accurate normalisation of small RNAs through new custom RT-qPCR arrays demonstrates Salmonella-induced microRNAs in human monocytes. BMC Genomics 2012; 13:23; PMID:22248082; http://dx.doi.org/10.1186/1471-2164-13-23.

31. Salvatori B, Iosue I, Djodji Damas N, Mangiavacchi A, Chiaretti S, Messina M, Padula F, Guarini A, Bozzoni I, Fazi F, et al. Critical Role of c-Myc in Acute Myeloid Leukemia Involving Direct Regulation of miR-26a and Histone Methyltransferase EZH2. Genes Cancer 2011; 2:585-92; PMID:21901171; http://dx.doi.org/10.1177/1947601911416357.

32. Ting Y, Medina DJ, Strair RK, Schaar DG. Differentiation-associated miR-22 represses Max expression and inhibits cell cycle progression. Biochem Biophys Res Commun 2010; 394:606-11; PMID:20214878; http://dx.doi.org/10.1016/j.bbrc.2010.03.030.

33. Studzinski GP, Bhandal AK, Brelvi ZS. Cell cycle sensitivity of HL-60 cells to the differentiation-inducing effects of 1-α,25-dihydroxyvitamin D3. Cancer Res 1985; 45:3898-905; PMID:3860289.

34. Renner AG, Dos Santos C, Recher C, Bailly C, Creancier L, Kruczynski A, Payrastre B, Manenti S. Polo-like kinase 1 is overexpressed in acute myeloid leukemia and its inhibition preferentially targets the proliferation

of leukemic cells. Blood 2009; 114:659-62; PMID:19458358; http://dx.doi.org/10.1182/blood-2008-12-195867.

35. Gjertsen BT, Schoffski P. Discovery and development of the Polo-like kinase inhibitor volasertib in cancer therapy. Leukemia 2014; 29(1):11-9

36. Vlachos IS, Kostoulas N, Vergoulis T, Georgakilas G, Reczko M, Maragkakis M, Paraskevopoulou MD, Prionidis K, Dalamagas T, Hatzigeorgiou AG. DIANA miRPath v.2.0: investigating the combinatorial effect of microRNAs in pathways. Nucleic Acids Res 2012; 40: W498-504; PMID:22649059; http://dx.doi.org/10.1093/nar/gks494.

37. Ceci M, Welshhans K, Ciotti MT, Brandi R, Parisi C, Paoletti F, Pistillo L, Bassell GJ, Cattaneo A. RACK1 is a ribosome scaffold protein for β-actin mRNA/ZBP1 complex. PloS one 2012; 7:e35034; PMID:22523568; http://dx.doi.org/10.1371/journal.pone.0035034.

38. Fontemaggi G, Dell'Orso S, Trisciuoglio D, Shay T, Melucci E, Fazi F, Terrenato I, Mottolese M, Muti P, Domany E, et al. The execution of the transcriptional axis mutant p53, E2F1 and ID4 promotes tumor neoangiogenesis. Nat Struct Mol Biol 2009; 16:1086-93; PMID:19783986; http://dx.doi.org/10.1038/nsmb.1669.

39. Tsafrir D, Tsafrir I, Ein-Dor L, Zuk O, Notterman DA, Domany E. Sorting points into neighborhoods (SPIN): data analysis and visualization by ordering distance matrices. Bioinformatics 2005; 21:2301-8; PMID:15722375; http://dx.doi.org/10.1093/bioinformatics/bti329.